

## Competition and coexistence of bond and charge orders in $(\text{TMTTF})_2\text{AsF}_6$

F. Zamborszky,<sup>1,2</sup> W. Yu,<sup>1</sup> W. Raas,<sup>1</sup> S. E. Brown,<sup>1</sup> B. Alavi,<sup>1</sup> C. A. Merlic,<sup>3</sup> and A. Baur<sup>3</sup>

<sup>1</sup>*Department of Physics and Astronomy, UCLA, Los Angeles, California 90095-1547*

<sup>2</sup>*Los Alamos National Laboratory, Los Alamos, New Mexico 87545*

<sup>3</sup>*Department of Chemistry and Biochemistry, UCLA, Los Angeles, California 90095-1569*

(Received 3 May 2002; revised manuscript received 1 July 2002; published 23 August 2002)

$(\text{TMTTF})_2\text{AsF}_6$  undergoes two phase transitions upon cooling from 300 K. At  $T_{CO}=103$  K a charge ordering (CO) occurs, and at  $T_{SP}(B=9\text{ T})=11$  K the material undergoes a spin-Peierls transition. Within the intermediate, CO phase, the charge disproportionation ratio is found to be at least 3:1 from  $^{13}\text{C}$  NMR  $T_1^{-1}$  measurements on spin-labeled samples. Above  $T_{SP}$  up to about  $3T_{SP}$   $T_1^{-1}$  is independent of temperature, indicative of low-dimensional magnetic correlations. With the application of about 0.15 GPa pressure,  $T_{SP}$  increases substantially, while  $T_{CO}$  is rapidly suppressed, demonstrating that the two orders are competing. The experiments are compared to results obtained from calculations on the one-dimensional extended Peierls-Hubbard model.

DOI: 10.1103/PhysRevB.66.081103

PACS number(s): 71.20.Rv, 71.30.+h, 71.45.Lr, 76.60.-k

Inhomogeneous charge and spin structures are a consequence of competing interactions and therefore of general interest in correlated electron systems. Examples include the high- $T_c$  cuprates<sup>1</sup> and manganites<sup>2</sup> as well as the quasi-two-dimensional (2D) organic conductors.<sup>3</sup> The quasi-1D salts made from TMTTF or TMTSF molecules are also susceptible to charge-ordered states. Independent of that, they are well known for the sequence of ground states accessible by applying pressure or selecting different counterions. For example, the material  $(\text{TMTTF})_2\text{PF}_6$  undergoes transitions from spin-Peierls (SP), antiferromagnetic, spin-density wave, and finally to superconducting ground states as the pressure is increased to 4–5 GPa.<sup>4,5</sup> For a long time, it was known that another phase transition occurs in a number of TMTTF salts with both centrosymmetric (e.g.,  $\text{AsF}_6$ ,  $\text{SbF}_6$ ) and non-centrosymmetric (e.g.,  $\text{ReO}_4$ ) counterions. Only recently<sup>6,7</sup> was the broken symmetry associated with this transition identified as a charge disproportionation.

In TMTTF salts the characteristic temperature of the onset of the charge-ordered (CO) phase is high, on the order of 100 K. It indicates that the interactions driving the charge ordering are relatively strong, and therefore potentially impact the electronic and magnetic properties of the disordered phase. Issues associated with CO correlations in these systems take particular relevance when considering that the nature of the metallic phase of TMTSF salts remains controversial.<sup>8–10</sup> Below we report the results of a number of NMR measurements on  $^{13}\text{C}$  spin-labeled samples of  $(\text{TMTTF})_2\text{AsF}_6$  in the CO phase. Our principle result is a mapping of the temperature/pressure phase diagram of the SP and CO phases that includes a tetracritical point with a region of coexistence of the two forms of order. There is good agreement between the experiments and the results of calculations on the 1D extended Hubbard<sup>11</sup> and Peierls-Hubbard models.<sup>12,13</sup>

A review of the characteristics of the CO phase and the phase transition is in order. With counterions  $\text{PF}_6$ ,  $\text{AsF}_6$ , and  $\text{SbF}_6$ , the ordering temperatures are 62 K, 103 K, and 154 K, respectively. Upon cooling, the salts made with the first two are already well into a region of thermally activated resistivities when the CO transition occurs. The last one undergoes a

continuous metal/semiconductor transition at  $T_{CO}$ . The mystery of the order parameter arose from the fact that no evidence for a superlattice was ever found with x-ray scattering. Charge order was identified as the proper description of the order parameter from NMR studies.<sup>7</sup> At high temperatures, the unit cell consists of two equivalent TMTTF molecules related by inversion about the counterion.<sup>14</sup> A low-frequency divergence of the real part of the dielectric susceptibility  $\chi_e$  is consistent with mean-field-like ferroelectric behavior.<sup>6,15</sup> The observations were taken as evidence for a breaking of the inversion symmetry within the unit cell, and the spontaneous dipole moment is associated with the charge imbalance on the two molecules.

All of the experiments were performed in  $B_0=9$  T magnetic field ( $^{13}\text{C}$  NMR frequency  $\nu=96.4$  MHz). Pressure was applied using a self-clamping BeCu cell, with Flourinert 75 serving as the pressure medium. The reproducible low-temperature pressure was calibrated in separate runs by measuring inductively the change of the superconducting transition temperature of lead. The NMR coil was constructed so that the molecular stacking axis (**a**) was oriented normal to the static magnetic field. Any significant reorientation about **a** between experimental runs is excluded by noting that the  $^{13}\text{C}$  internuclear dipolar coupling remained unchanged.

In Fig. 1 we show the temperature dependence of the relative hyperfine shifts for all of the unique  $^{13}\text{C}$  sites. Once the molecules are inside the solid, the two sites forming the bridge are inequivalent and have different hyperfine shifts. At high temperatures the two molecules within the unit cell are equivalent. Below the phase transition at  $T_{CO}=103$  K, each of the two lines splits into two peaks with equal absorption strengths. We showed this to be a result of a charge disproportionation developing between two inequivalent molecules, and the order-parameter amplitude is proportional to the difference of the NMR frequencies within each of the split lines. The character of the transition is second order.

The amplitude of the charge disproportionation can be estimated from the spin-lattice relaxation rates. These are shown in Fig. 2. The relaxation rates are about one order-of-magnitude faster on one of the two types of molecules. Ide-

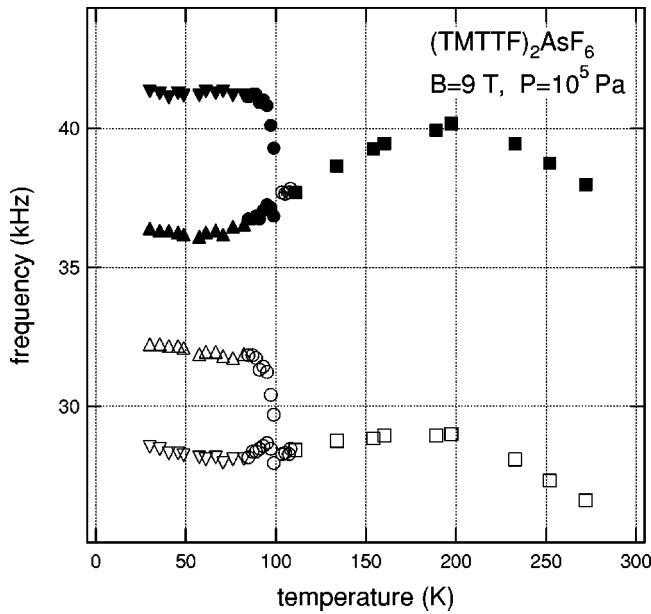


FIG. 1. Positions of the  $^{13}\text{C}$  NMR peaks versus temperature at the magic angle at ambient pressure for  $(\text{TMTTF})_2\text{AsF}_6$ . The CO transition takes place at  $T_{CO}=103$  K.

ally, we expect that  $T_1^{-1}$ , dominated by hyperfine coupling, is proportional to the electronic density on a particular molecule. For isotropic hyperfine interaction and no spectral overlap whatsoever between the respective absorption lines,  $T_1^{-1} \propto \rho^2$ , with  $\rho$  the molecular charge count. Neither one of these conditions is strictly true here, so the ratio of the relaxation rates of sites on the high- and low-density mol-

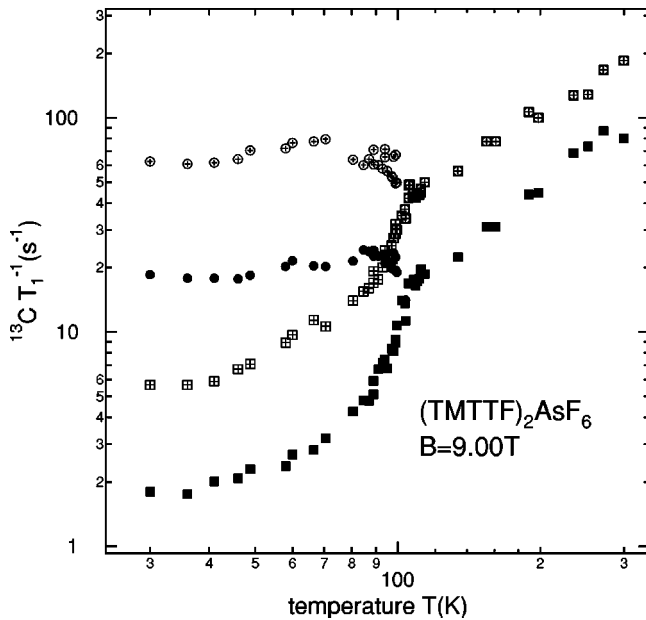


FIG. 2.  $^{13}\text{C}T_1^{-1}$  relaxation rate as a function of temperature at ambient pressure in  $(\text{TMTTF})_2\text{AsF}_6$ . Spectra were taken at the magic angle, and the magnetization recovery was obtained by integrating over the distinct peaks of the absorption spectra. Similar markers represent  $^{13}\text{C}T_1^{-1}$  of peaks evolving from the same high-temperature peak.

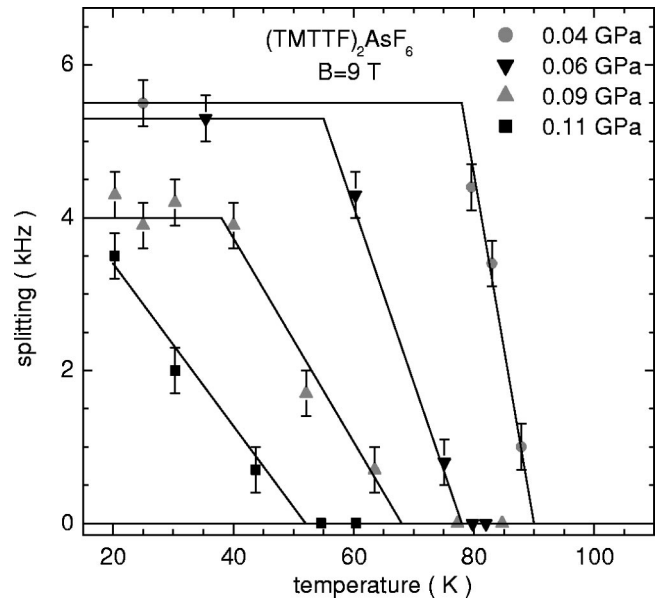


FIG. 3. The order parameter as a function of temperature at various pressures. The solid lines are to guide the eye.

ecules determines a *lower bound* for the disproportionation, namely, 3:1.

Modest applied pressures strongly depress  $T_{CO}$ . The order parameter of the CO phase, taken from the temperature dependence of the splitting of the NMR lines, is shown in Fig. 3 at different pressures. Three effects are visible as the pressure is increased: (i) The maximum splitting is decreased, (ii)  $T_{CO}$  is decreased, and (iii) the order parameter develops much less steeply. Our experimental technique does not have enough resolution close to  $T_{CO}$  where the critical behavior of the order parameter should follow theoretical predictions. The low-pressure data is consistent with the mean-field critical exponent ( $\beta=0.5$ ) down to 10–15 K from  $T_{CO}$ , in accordance with the observed Curie law of the dielectric constant in the same temperature regime.<sup>6</sup> At higher pressures, as  $T_{CO}$  gets smaller, the classical scaling regime is expected to shrink. Our data clearly show a deviation from the classical behavior. We can draw two possible scenarios: (i) the critical behavior is crossing over to a quantum limit with a critical exponent increasing towards  $\beta=1$ , as was observed in pressurized  $(\text{Ba}_x\text{Sr}_{1-x})\text{TiO}_3$  ferroelectrics.<sup>16</sup> (ii) The observations result from coupling between the different orders.

$T_{SP}$  is identified from the temperature dependence of either  $^{13}\text{C}$  or  $^{75}\text{As}T_1^{-1}$ .  $^{13}\text{C}$  is a spin  $I=1/2$  nucleus for which  $T_1^{-1}$  falls precipitously below  $T_{SP}$ .  $^{75}\text{As}$ , on the other hand, has spin  $I=3/2$ , so it couples to electric-field gradient fluctuations produced, for example, by lattice vibrations. The peak in  $^{75}\text{As}T_1^{-1}$  at  $T_{SP}$  is naturally associated with the critical slowing down of the soft  $2k_F$  phonons.<sup>17</sup> The completed phase diagram for  $(\text{TMTTF})_2\text{AsF}_6$  appears in Fig. 4. The CO phase diminishes quite rapidly:  $P=P_c \leq 0.15$  GPa is enough to suppress it.

The phase diagram has a remarkable feature: while  $T_{CO}$  is decreasing,  $T_{SP}$  increases significantly up to about 150% of its ambient pressure value. After the charge ordering is sup-

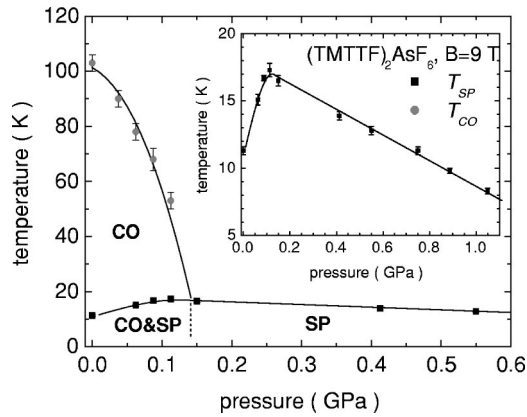


FIG. 4. Phase diagram of  $(\text{TMTTF})_2\text{AsF}_6$  established from NMR experiments at  $B=9$  T. The lines are a guide to the eye. The dashed line is used only to emphasize that a region of coexistence is present.

pressed at  $P_c$ ,  $T_{SP}$  decreases weakly with additional pressure. The maximum of  $T_{SP}$  at  $P_c$  indicates that the CO site order and the SP bond order are competing. If the competition is sufficiently weak, the order parameters will coexist. Otherwise, a first-order transition line divides the two phases. In principle, the CO and SP order parameters could be simultaneously characterized by x-ray scattering experiments. To date, we are not aware of a published x-ray report of the CO phase, even at ambient pressure. We call attention to this not only because NMR is a local probe, but also because the methods described above for determining the CO order parameter do not work in the SP phase. This is because the paramagnetic shifts are nearly absent for the singlet ground state and all  $^{13}\text{C}$  sites are equivalent. There is an exception: magnetic fields  $B$  larger than a critical value  $B_c$  produce an incommensurate phase, through the generation of triplet excitations. In a 1D picture, the triplets consist of soliton/antisoliton pairs. Typically  $B_c \propto T_{SP}$ . Although it is not measured for  $(\text{TMTTF})_2\text{AsF}_6$ , we know that  $B_c = 19$  T for the  $\text{PF}_6$  salt.<sup>18</sup> Applied fields greater than 19 T resulted in broadened NMR lines associated with the staggered spin density of the excitations.<sup>19</sup> Line shapes demonstrating the effect near to  $B_c$  are shown in Fig. 5. At low fields, we see a single line showing that all  $^{13}\text{C}$  sites are equivalent in the SP phase. If the charge ordering is still present, we expect the absorption at high fields to consist of exactly four contributions all of which are identical. Two contributions are expected without the charge ordering. Four *well-separated* “ledges” are evident on each side of the maximum at the higher field, which we interpret as coming from the nuclei near the center of the solitonlike excitations where the staggered spin density is maximum.<sup>20,21</sup> The substantial differences in hyperfine fields on the four sites indicate that the disproportionation remains large even in the ground state, i.e., the two orders coexist as shown in Fig. 4. A smaller charge disproportionation is also expected in the SP phase<sup>13</sup> at high pressures, but our experimental setup did not allow to investigate it.

We should emphasize that the 1D extended Peierls-Hubbard model contains most of the essential physics that

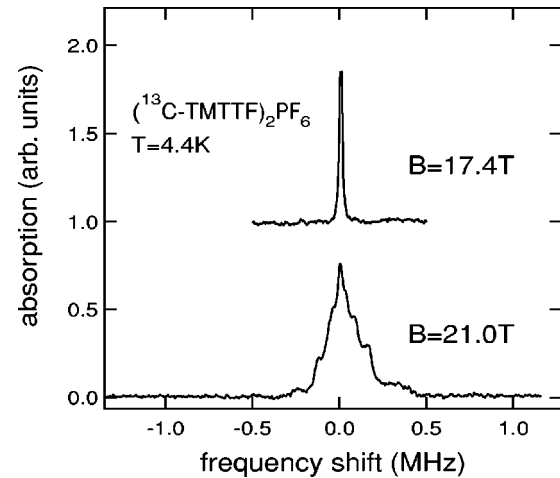


FIG. 5.  $^{13}\text{C}$  NMR line shapes of  $(\text{TMTTF})_2\text{PF}_6$  at fields close to the critical field  $B_c$ , at ambient pressure. The broadening for  $B > B_c$  is characteristic of the incommensurate phase.

produces the observed phase diagram. Justification for a quasi-1D point of view follows from the fact that the molecular spacing along the stack alternates.<sup>14</sup> It can be modeled by introducing intrachain hopping integrals  $t_1$  and  $t_2$  along the stack. Therefore, the system is half-filled and electron-electron Umklapp scattering in one dimension opens a charge gap  $\Delta_\rho$ .<sup>22</sup> Provided that  $\Delta_\rho \gg t_\perp$ , where  $t_\perp$  is the transverse hopping, 1D confinement leads to an insulating state even at high temperatures and at  $T > T_{CO}$ .

Without phonon coupling, the 1D extended Hubbard model will produce a CO state if the Coulomb interaction is sufficiently large and long ranged,<sup>22</sup> i.e., the nearest-neighbor interaction  $V > V_c$ .<sup>11</sup> In the TMTTF salts, it is expected that  $V$  is very close to the predicted threshold obtained in strong-coupling perturbation theory.<sup>13,23</sup> Further, the large lower bound that we infer for the charge disproportionation is quantitatively reasonable when compared to model parameters.<sup>11,13</sup> The principle effect of pressure is to increase the hopping integrals, which leads to a rapid destabilization of the CO phase, just as we observe.  $P > P_c$  results in a SP ground state, once the phonon coupling is included.

Regarding the high-temperature CO phase, there are two qualitative differences between recent numerical works and our experimental observations. One of them is the expectation that the charge ordering occurs together with the metal-insulator transition.<sup>13</sup> The other is the character of the transition. The measurements are consistent with the CO phase transition being a continuous one along the entire line, whereas *mean-field* calculations describe the transition as first order. Including the dimerization of the 1D stack is known to eliminate the first-order character in the mean-field calculations of the 1D extended Hubbard model.<sup>11</sup> Therefore, it is very likely that the dimerization is crucial in *three* respects. First, it confines coherent charge motion to the stacks and because of this it is appropriate to compare to 1D models. Second, the confinement assures that a metal-insulator crossover occurs at a high temperature, perhaps far above  $T_{CO}$ . Third, it changes the character of the CO transition from first order to second order.

Returning to the issue of metal vs insulator in the TMTTF salts, we mention that even though the CO transition takes place within the insulating phase in  $\text{PF}_6$  and  $\text{AsF}_6$ , there is a signature of the transition in the electrical conductivity.<sup>24</sup> However there is one choice of centrosymmetric counterion,  $\text{SbF}_6$ , which undergoes a real transition to an insulating state at  $T_{CO}$ .<sup>24</sup> This unique feature cannot be understood easily, since the high-temperature band-structure parameters are quite similar to  $\text{PF}_6$  and  $\text{AsF}_6$ .<sup>25</sup> The  $\text{SbF}_6$  has a more compact packing in the **bc** plane, leading to a more pronounced stack-counterion interaction. This can have an impact on the dimensionality, which has not been taken into account in the theoretical models yet.

In conclusion, we studied the pressure dependence of the relative stability of the CO and SP phases observed in  $(\text{TMTTF})_2\text{AsF}_6$  using  $^{13}\text{C}$  NMR spectroscopy and spin-

lattice relaxation measurements. The coexistence of the two orders was established along with the existence of a tetra-critical point in the temperature/pressure phase diagram. The CO phase is suppressed easily with modest pressure; the natural interpretation is that it results from the effect of the increasing bandwidth relative to the strength of the near-neighbor Coulomb repulsion  $V$  within the stacks. The lower bound for the charge disproportionation is set at 3:1. The phase diagram and disproportionation amplitude are consistently compared to results of calculations on the 1D extended Hubbard and Peierls-Hubbard models.

The work was supported by the National Science Foundation under Grant No. DMR-9971530. We would like to acknowledge helpful discussions with S. Brazovskii, R. T. Clay, S. Kivelson, and S. Mazumdar.

- 
- <sup>1</sup>J.M. Tranquada, B.J. Sternlieb, J.D. Axe, Y. Nakamura, and S. Uchida, *Nature (London)* **375**, 561 (1995).  
<sup>2</sup>S. Mori, C.H. Chen, and S.W. Cheong, *Nature (London)* **392**, 473 (1998).  
<sup>3</sup>K. Miyagawa, A. Kawamoto, and K. Kanoda, *Phys. Rev. B* **62**, R7679 (2000).  
<sup>4</sup>T. Acahi, O. E., K. Kato, H. Kobayashi, T. Miyazaki, M. Tokumoto, and A. Kobayashi, *J. Am. Chem. Soc.* **122**, 3238 (2000).  
<sup>5</sup>H. Wilhelm, D. Jaccard, R. Duprat, C. Bourbonnais, D. Jérôme, J. Moser, C. Carcel, and J.M. Fabre, *Eur. Phys. J. B* **21**, 175 (2001).  
<sup>6</sup>F. Nad, P. Monceau, C. Carcel, and J.M. Fabre, *Phys. Rev. B* **62**, 1753 (2000).  
<sup>7</sup>D.S. Chow, F. Zamborszky, B. Alavi, D.J. Tantillo, A. Baur, C.A. Merlic, and S.E. Brown, *Phys. Rev. Lett.* **85**, 1698 (2000).  
<sup>8</sup>D. Jerome *et al.*, *Synth. Met.* **70**, 719 (1995).  
<sup>9</sup>L.D. Vescoli, L. Degiorgi, W. Henderson, G. Gruner, K.P. Starkey, and L.K. Montgomery, *Science* **281**, 1181 (1998).  
<sup>10</sup>G. Mihaly, I. Kezsmarki, F. Zamborszky, and L. Forro, *Phys. Rev. Lett.* **84**, 2670 (2000).  
<sup>11</sup>H. Seo and H. Fukuyama, *J. Phys. Soc. Jpn.* **66**, 1249 (1997).  
<sup>12</sup>S. Mazumdar, R.T. Clay, and D.K. Campbell, *Phys. Rev. B* **62**, 13400 (2000).  
<sup>13</sup>R.T. Clay, S. Mazumdar, and D.K. Campbell, cond-mat/0112278 (unpublished).  
<sup>14</sup>J.P. Pouget and S. Ravy, *J. Phys. I* **6**, 1501 (1996).  
<sup>15</sup>P. Monceau, F.Y. Nad, and S. Brazovskii, *Phys. Rev. Lett.* **86**, 4080 (2001).  
<sup>16</sup>P. Roth, E. Hegenbarth, M. Müller, and U. Escher, *Ferroelectrics* **74**, 331 (1987).  
<sup>17</sup>S. E. Brown (unpublished).  
<sup>18</sup>S.E. Brown, W.G. Clark, F. Zamborszky, B.J. Klemme, G. Kriza, B. Alavi, C. Merlic, P. Kuhns, and W. Moulton, *Phys. Rev. Lett.* **80**, 5429 (1998).  
<sup>19</sup>S.E. Brown, W.G. Clark, B. Alavi, D.S. Chow, C.A. Merlic, and D.J. Tantillo, *Synth. Met.* **103**, 2056 (1999).  
<sup>20</sup>T.W. Hijmans, H.B. Brom, and L.J. de Jongh, *Phys. Rev. Lett.* **54**, 1714 (1985).  
<sup>21</sup>Y. Fagot-Revurat, M. Horvatić, C. Berthier, P. Ségransan, G. Dhalenne, and A. Revcolevschi, *Phys. Rev. Lett.* **77**, 1861 (1996).  
<sup>22</sup>V.J. Emery, R. Bruinsma, and S. Barisić, *Phys. Rev. Lett.* **48**, 1039 (1982).  
<sup>23</sup>F. Mila, *Phys. Rev. B* **52**, 4788 (1996).  
<sup>24</sup>R. Laversanne, C. Coulon, B. Gallois, J.P. Pouget, and R. Moret, *J. Phys. Lett.* **45**, L393 (1984).  
<sup>25</sup>T. Granier, B. Gallois, A. Fritsch, L. Ducasse, and C. Coulon, in *Lower-Dimensional Systems and Molecular Electronics*, Vol. 248 of NATO Advanced Studies Institute, edited by R. M. Metzger, Series B-Physics (Plenum, New York, 1990).